Small Angle Neutron Scattering Studies of Vesicle Stability

Joseph T. Mang and Rex P. Hjelm

MLNSC, Los Alamos National Laboratory, Los Alamos, NM 87545-1663 USA.

Abstract

Small angle neutron scattering (SANS) was used to investigate the structure of mixed colloids of egg yolk phosphatidylcholine (EYPC) with the bile salt, cholylglycine (CG), in D_2O as a function of pressure (P) and temperature (T). At atmospheric pressure, the system forms an isotropic phase of mixed, single bilayer vesicles (SLV's). Increasing the external hydrostatic pressure brought about significant changes in particle morphology. At T = 25 ^{o}C, application of a pressure of 3.5 MPa resulted in the collapse of the SLV's. Further increase of P, up to 51.8 MPa, resulted in a transition from a phase of ordered (stacked), collapsed vesicles to one of stacked, ribbon-like particles. A similar collapse of the vesicles was observed at higher temperature (T = 37 ^{o}C) with increasing P, but at this temperature, no ribbon phase was found at the highest pressure explored.

KEY WORDS : pressure, small angle neutron scattering, stability, vesicles.

1. INTRODUCTION

In recent years, there has been considerable interest into the stability of bilayer vesicles formed by mixed surfactant systems [1-3]. This work has largely considered the effects of packing due to molecular geometrical factors and the effect of the bending elastic modulus. This assumption is embodied in the work of Israelachvilli [4] and also of Safran, Pincus *et al.* [1]. In the latter work, Safran and Pincus considered the curvature free energy and showed that, with the introduction of a second molecular species the composition of each monolayer of the bilayer provides an additional degree of freedom that can give rise to effective negative values of the curvature free energy for vesicles, making them stable with respect to flat lamellae. These studies consider mixed bilayers as incompressible; thus the effects of pressure on vesicle stability is not explicitly considered. The expression for the free energy for shapes of closed fluid lipid-bilayer membranes, including vesicles relative to planar lamellae derived by Helfrich [5] as well as others includes pressure as well as the energy of curvature,

$$F_c = \frac{1}{2} K_c \int (c_1 + c_2 - c_o)^2 \, dA + \Delta p \int dV + \gamma' \int dA . \qquad (1)$$

Here, K_c is the bending modulus, c_1 and c_2 the principle curvatures of the interface and c_o the spontaneous curvature. Δp (= p_i - p_e) represents a pressure gradient between the interior of the membrane and the surrounding fluid while γ' represents the surface tension or surface energy density. In this model, the pressure gradient plays an integral role in determining particle stability. For example, in considering a simple particle morphology such as a spherical vesicle of average curvature R^{-1}, minimization of F_c requires,

$$\Delta p \sim \frac{2\gamma'}{R},$$

which is just the classic Young-Laplace (Y-L) equation for soap bubbles.

While the Helfrich equation (Eq. 1) has been successful in predicting the equilibrium shapes of membrane systems, there has been considerable controversy [4,6-7] into the physical origin of the last two terms which appear in the expression. These terms enter into the Helfrich formalism as Lagrange multipliers to satisfy the conditions of constant volume and area, but they may represent real work contributions to the free energy. This result, however, was originally derived to describe macroscopic systems, and as Tanford [6] originally pointed out vesicles are permeable to water; thus it is difficult to understand how a hydrostatic pressure gradient can be maintained. So too is the possibility of an osmotic gradient which would require an excess amount of solute (salt, for example) to be trapped at the interior. While a small gradient may be possible when the vesicles are formed by mechanical means (sonification), such a gradient is unlikely when the vesicles form spontaneously as in the present case. Further, it is unclear whether such concepts as surface tension apply on the microscopic level [8,9].

Mixed surfactant systems form vesicles of definite size and shape. If there is no pressure gradient across the curved interface, and there is no surface tension, then what holds these membranes together? We may not be able to define a surface tension or a pressure gradient in the macroscopic sense for these systems, however, the forces involved in binding the membranes may appear as effective pressures and surface tensions. So, while the mathematical formalism is sound, a reinterpretation of the work terms may be needed.

In studying the stability of membrane systems then, it is important to be able to quantify these forces no matter what their origin. By varying the external hydrostatic pressure according to the Y-L interpretation we may reach a point where the applied pressure exceeds the effective pressure of the membranes, forcing them to collapse. The point of collapse then will provide valuable information on the magnitude of the forces which act on these systems. In order to elucidate the role of pressure in determining the stability criteria for colloids of

mixed surfactant systems, we performed small-angle neutron scattering (SANS) measurements on particle morphology as a function of pressure of bile salt (cholylglycine)/egg yolk phosphatidylcholine (EYPC) mixtures in the region of the isotropic (*I*) phase.

2. MATERIALS AND METHODS

2.1 System

CG/EYPC samples were prepared by dissolving purified EYPC (Sigma, type VIII-E) and Sodium glycocholate (Sigma Chemical Co.) in ethanol and then mixing the two components in the molar ratio (EYPC/BS) of $\Gamma^{-1} = 0.8$. After vacuum drying, the preparation was dissolved in a D_2O buffer containing 0.15 M NaCl with tris buffer (pH 7.5) to make a stock solution containing 50 mg/ml total lipid concentration. The samples (2 mg/ml) were prepared by further dilution with D_2O buffer and allowed to equilibrate for ~ 2 days in the dark. The final concentration corresponded to the mixed, spherical single bilayer vesicle (SLV) portion of the phase diagram.

2.2 Small Angle Neutron Scattering

SANS measurements were performed at the Intense Pulsed Neutron Source at Argonne National Laboratory, employing the Small-Angle Neutron Diffractometer (SAD) and at the Cold Neutron Research Facility (CNRF) of the National Institute of Standards and Technology (NIST), employing the NG3 beamline. On SAD, scattering data were acquired using the time-of-flight method [10]. At NIST, neutrons of wavelength 5 Å ($\Delta\lambda/\lambda = 0.15$)

and two different camera settings were used. In both cases, the raw data were corrected for empty cell, background and buffer scattering. In order to interpret the data, a nonlinear least squares procedure was used to fit the measured lineshapes to the expected scattering of different model systems.

Neutron scattering experiments measure the scattering intensity, I(Q), as the absolute differential cross section per unit scattering mass (cm^2 mg^{-1}) as a function of the magnitude of the scattering vector, Q, which is related to the incident neutron wavelength, λ, and the scattering angle, 2θ, by $Q = (4\pi/\lambda) \sin\theta$. The scattered neutron intensity, for a system of N particles of volume, V, and uniform scattering length density, dispersed in a uniform solvent, can be expressed as :

$$I(Q) = \frac{N}{M} V^2 (\Delta\rho)^2 \langle P(\mathbf{Q}) S(\mathbf{Q}) \rangle,$$

where P(**Q**) is the normalized form factor of a single particle and is given as $P(\mathbf{Q}) = |F(\mathbf{Q})|^2$. F(**Q**) is the Fourier transform of the particle structure given as the variation of scattering length density, $\rho(\mathbf{r})$, as a function of position, r, in the sample. S(**Q**) is the structure factor which accounts for interparticle correlations and M is the mass of the particle. $\Delta\rho$ is the scattering length density contrast between the average scattering length density of the particle, $\overline{\rho_p}$, and solvent, ρ_s, $\Delta\rho = \overline{\rho_p} - \rho_s$. The particle form factors which are relevant to this work are summarized in Table I.

3. RESULTS

The results of SANS measurements of the CG/EYPC system over the range of pressures explored at T = 25 ^{o}C are shown in figure 1, where the curves have been shifted

along the vertical axis for clarity. Dramatic changes in the measured scattering curves were seen with increasing pressure. At atmospheric pressure (P = 0.1 MPa), the data are consistent with the presence of mixed SLV's, as expected from the known phase diagram [11]. At elevated pressures there is the appearance of a Bragg peak centered at Q_o = 0.123 $Å^{-1}$ (1.23 nM^{-1}), corresponding to a bilayer spacing, d, of 51 Å. Pressure-dependent changes were observed in the fall-off at low-Q. The appearance of the single Bragg peak suggests the presence of stacking order in the system at high pressure, while the change in slope of the low-Q data suggests a change in the fundamental stacked unit with pressure.

Results of model calculations along with the measured data are shown in Fig. 2 for several different pressures. As seen in Fig. 2a, the data obtained at atmospheric pressure can be readily modeled as a system of mixed SLV's. The solid line in Fig. 2a is the result of a fit of the data to the particle form factor for an SLV with R = 147 Å and thickness, t = 35 Å. Deviations of the model from the measured data at the minima are likely due to a small amount of polydispersity and or multiple scattering. The solid line in Fig. 2d is the result of a fit of the data to a model consisting of stacked infinite ribbon-like (SR) particles, 30 Å thick, 25 Å wide and with a stack height, M, of 13. Attempts to model the data as stacks of infinite sheets failed to accurately describe our data as randomly-oriented infinite sheet scattering falls-off as Q^{-4} at low-Q and produces a Bragg peak that is several orders of magnitude too small. At the intermediate pressures, the slopes of the scattering curves in the low-Q region suggest a coexistence region of ribbons with infinite sheets. In figures 2b and 2c, the solid lines are the result of fits of the data to a linear combination of the SLV, SR and stacked infinite sheet (SS) models. Best fits were obtained with infinite sheets of 30 Å thickness. At P = 3.5 MPa, M = 5, while for higher pressures, M = 13 gave the best results. Such a coexistence has been seen previously in electron micrograph studies of native bile [12].

Scattering curves measured at 37 ^{o}C as a function of pressure are shown in figure 3. As in the previous data, significant changes occurred upon increasing pressure. For P < 5.0

MPa, (Fig. 3) the data is well described by the form factor for an SLV with R = 170 Å and t = 40 Å. At higher pressures, the curves fall off more rapidly in the low-Q region, while the maxima arising from the SLV contribution decreased. For all pressures, the scattering curves overlay above Q = 0.04 $Å^{-1}$. This suggests that the transition is not complete and that the contribution from the new phase, while dominating at low-Q, falls off quickly.

The value of ~ 2 for the slope at low-Q, again suggests the presence of sheet-like structures. But in contrast to the data collected at T = 25 ^{o}C, no distinct Bragg peak is seen in the curves at high pressure. Only a slight inflection in the scattering curve is visible, centered at Q_o = 0.126 $Å^{-1}$. The solid lines in figure 3, for pressures above 5.0 MPa, are the results of model calculations consisting of SLV's, SS's and simple sheet-like structures. Initial attempts to model the data as SLV's + SS's or SLV's + sheets, alone, failed as, while both models describe the data well in the low-Q region, the former falls off too quickly and the latter too slowly in the region Q > 0.012 $Å^{-1}$. For all fits shown in figure 3, the radius of the vesicle was held constant at 170 Å and the thickness of the vesicle fixed at 40 Å. For the sheet-like structures, the best fits were obtained with a sheet thickness of 38 Å with d = 50 Å. Slightly better fits were obtained at the higher pressures by increasing the stack height of the SS phase from 6 to 10.

Figure 4 shows a plot of the zero angle intensity contribution from the SLV phase as a function of pressure for both temperatures. In both cases, the contribution from the SLV phase decreased rapidly with increasing pressure, indicative of vesicle collapse. The finer steps in pressure at 37 ^{o}C demonstrates the abrupt collapse clearly, as the SLV phase contribution decreased by 43 % in raising P from 2.0 to 5.0 MPa.

4. DISCUSSION

The observed pressure-dependent changes in the bile salt/EYPC particle morphology implies that work can be done on them. This provides insight into the factors that stabilize the particle shapes. At both temperatures studied, evidence of vesicle collapse is apparent in the measured lineshapes with increasing pressure. The collapse of the vesicles suggests that the applied pressure exceeded the effective pressure of the vesicles as described previously. If we model the effective pressure according to the Y-L equation, using a nominal value of 50 mN/M for γ' and an average value of R of 159 Å, we calculate a Δp of ~ 6.3 MPa. As seen in figure 4, this is very close to the pressure at which the contribution, to the overall scattering, from the vesicle phase becomes insignificant. Thus, even if it is unlikely that a hydrostatic or osmotic pressure gradient exists in vesicles, the shape is stabilized by an apparent pressure that behaves something like that predicted by the Y-L equation.

At pressures above 6.9 MPa, we see the formation of ribbon-like particles at 25 ^{o}C. The ribbon-like structure can arise from discrete particles or from defects in lamellar layers as are found in some other liquid crystalline systems [13]. In either case, the formation of such anisotropic structures would require a redistribution of the bile salt from the interior of the bilayer to the edges, thus stabilizing the ribbon phase by shielding the EYPC tails from contact with water. The anisotropic form of the ribbon phase indicates a strong tendency of the bile salt to associate with the EYPC tail as opposed to being in solution. Such a pressure-driven re-arrangement implies a significant volume change associated with the removal of bile salt from the bilayer interior to the bilayer edge. This arrangement is not unprecedented as in the ribbon phase of the potassium palmitate/potassium laurate/water system [14], the shorter tailed monomers (potassium laurate) are found to segregate to the exterior surfaces of the ribbons.

The presence of bile salt at the ribbon edges is consistent with the molar ratio of BS to EYPC. The lack of a ribbon phase in the CG/EYPC system at 37 ^{o}C may be anticipated with an increased solution solubility of the bile salt component at the higher temperature [15].

With the bile salt preferring to be associated with the water phase, the ribbon-like structures cannot be supported, leading to the observed infinite sheet-like structures. Also, at the higher temperature, there is likely an increase in membrane fluctuations which can prevent stacking.

5. CONCLUSION

Using small angle neutron scattering, we have studied the aggregate structure in the isotropic phase of the CG/EYPC system as a function of pressure. At T = 25 ^{o}C, upon increasing the external hydrostatic pressure, a transition from an isotropic phase of discrete particles to an ordered phase was observed. At the highest pressures investigated, the CG/EYPC was found to transform to a ribbon phase. At T = 37 ^{o}C, a similar behavior was seen with increasing pressure. However, no ribbon phase was found at the highest pressure studied. The observed collapse of the SLV's with increasing pressure is consistent with the Y-L model. Additional measurements are needed in order to clarify the nature of the pressure gradient across the curved surfaces of the colloids formed by the GC/EYPC system.

REFERENCES

1. S. A. Safran, P. A. Pincus, D. Andelman and F. C. MacKintosh, *Phys. Rev.* **A43**: 1071 (1991).
2. R. Bruinsma, M. Goulian and P. Pincus, *Biophys. J.* **67**:746 (1994).
3. M. M. Kozlov and V. S. Markin, J. Phys. (*France*) **51**:559 (1990).
4. J. Israelachvili, Intermolecular and Surface Forces (Academic Press, London, 1985).
5. O. Zhong-can and W. Helfrich, *Phys. Rev.* **A39**:5280 (1989).
6. C. Tanford, *Proc. Natl. Acad. Sci.* **76**:3318 (1979).
7. S. H. White, *Proc. Natl. Acad. Sci.* **77**:4048 (1980).
8. S. E. Feller and R. W. Pastor, *Biophys. J.* **71**:1350 (1996).
9. F. Jahnig, *Biophys. J.* **71**:1348 (1996).
10. R. P. Hjelm, *J. Appl. Cryst.* **21**:618 (1988).
11. R. P. Hjelm, H. Alkan and P. Thiyagarajan, *Mol. Cryst. Liq. Cryst.* **180A**:155 (1990).
12. S. Corradini, G. Arancia, A. Calcabrini, P. Guardia, L. Baiocchi, A. Nistri, L. Giacomelli and M. Angelico, *Journal of Heptology* **22**:642 (1995).
13. M. C. Holmes, M . S. Leaver and A. M. Smith, *Langmuir* **11**:356 (1995), and references therein.
14. G. Chidichimo, A. Golemme, J. W. Doane and P. Westerman, *J. Chem. Phys.* **82**: 536 (1985).
15. J. T. Mang and R. P. Hjelm, *Mol. Cryst. Liq. Cryst.*, in press.

Table I : Particle form factors for the structural models used in this study

Model	Particle Form Factor, P(**Q**)
single layer vesicle	$\frac{9}{Q^2(R^3-r^3)^2}[R^2 j_1(QR)-r^2 j_1(Qr)]^2$
infinite sheet	$\frac{P_z(Q)}{Q^2}$, $F_z(\mathrm{Q}) \equiv [\frac{2l\Delta\rho_H}{L\overline{\Delta\rho}}\,\mathrm{sinc(Ql)} + \frac{2l_T\Delta\rho_{TH}}{L\overline{\Delta\rho}}\,\mathrm{sinc(Ql_T)}]$
infinite ribbon	$\frac{\lvert F_z(Q_k)\sin c(Q_l l_y)\rvert^2}{Q_l}$

Figure Captions

Figure 1 : SANS measurements of the CG/EYPC system (EYPC/BS = 0.8, 2mg/ml) as a function of pressure.

Figure 2 : SANS measurements as a function of pressure (T = 25 ^{o}C). The solid lines are fits to model systems as described in the text. With increasing pressure, the system transformed from an isotropic phase of SLV's to a phase of stacked ribbon-like particles.

Figure 3 : Measured line shapes of the CG/EYPC system as a function of pressure at T = 37 ^{o}C.

Figure 4 : Zero angle intensity contribution from the SLV phase as a function of P and T. The rapid decrease in the contribution is indicative of vesicle collapse.

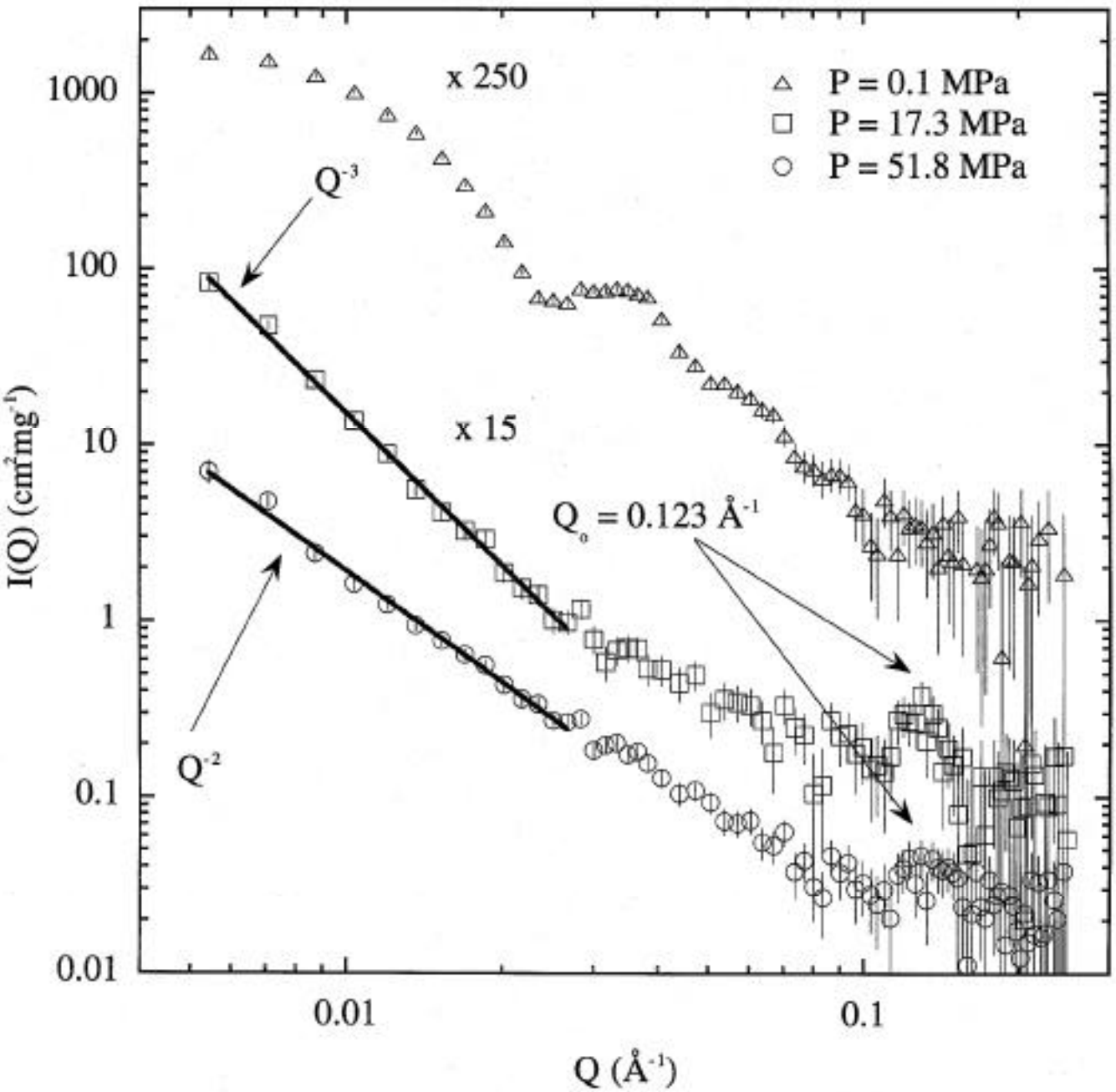
x 250
P = 0.1 MPa
P = 17.3 MPa
P = 51.8 MPa
Q^-3
x 15
Q_o = 0.123 Å^-1
Q^-2
1000
100
10
1
0.1
0.01
I(Q) (cm^2mg^-1)
0.01
0.1
Q (Å^-1)

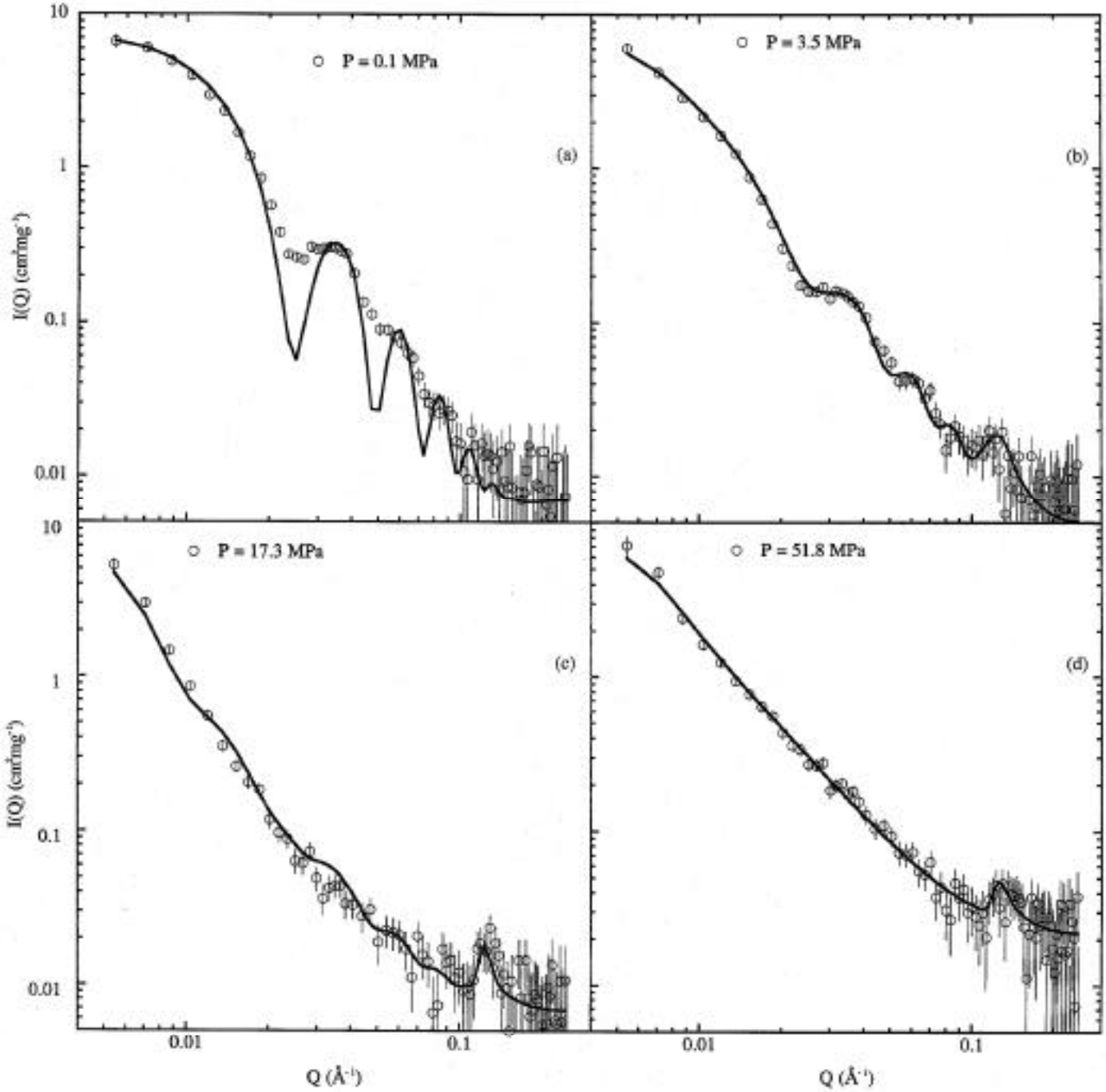
P = 0.1 MPa
(a)
P = 3.5 MPa
(b)
P = 17.3 MPa
(c)
P = 51.8 MPa
(d)
I(Q) (cm²mg⁻¹)
Q (Å⁻¹)
10
1
0.1
0.01
0.01
0.1

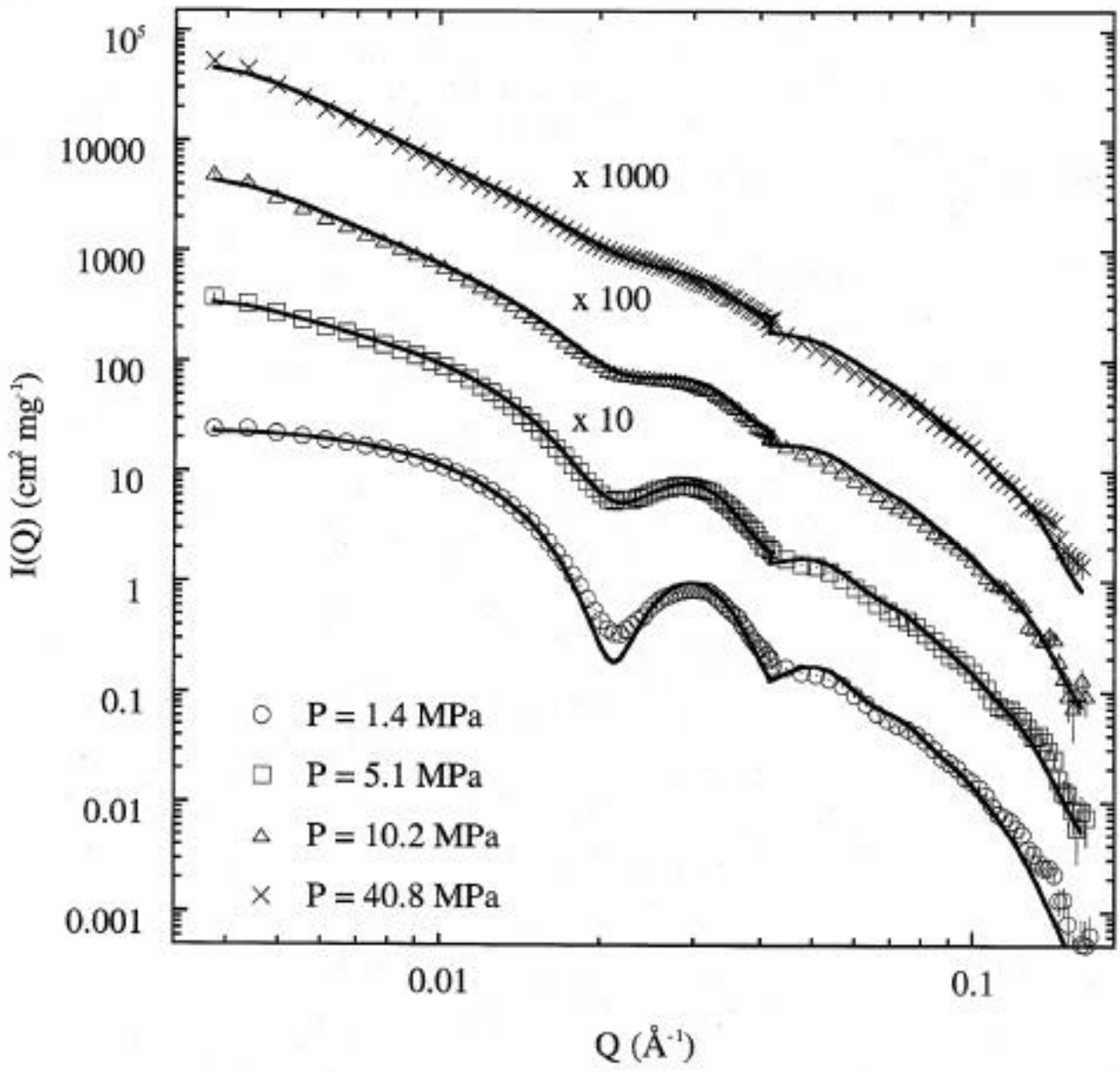
10^5
10000
1000
100
10
1
0.1
0.01
0.001
I(Q) (cm^2 mg^-1)
x 1000
x 100
x 10
P = 1.4 MPa
P = 5.1 MPa
P = 10.2 MPa
P = 40.8 MPa
0.01
0.1
Q (Å^-1)

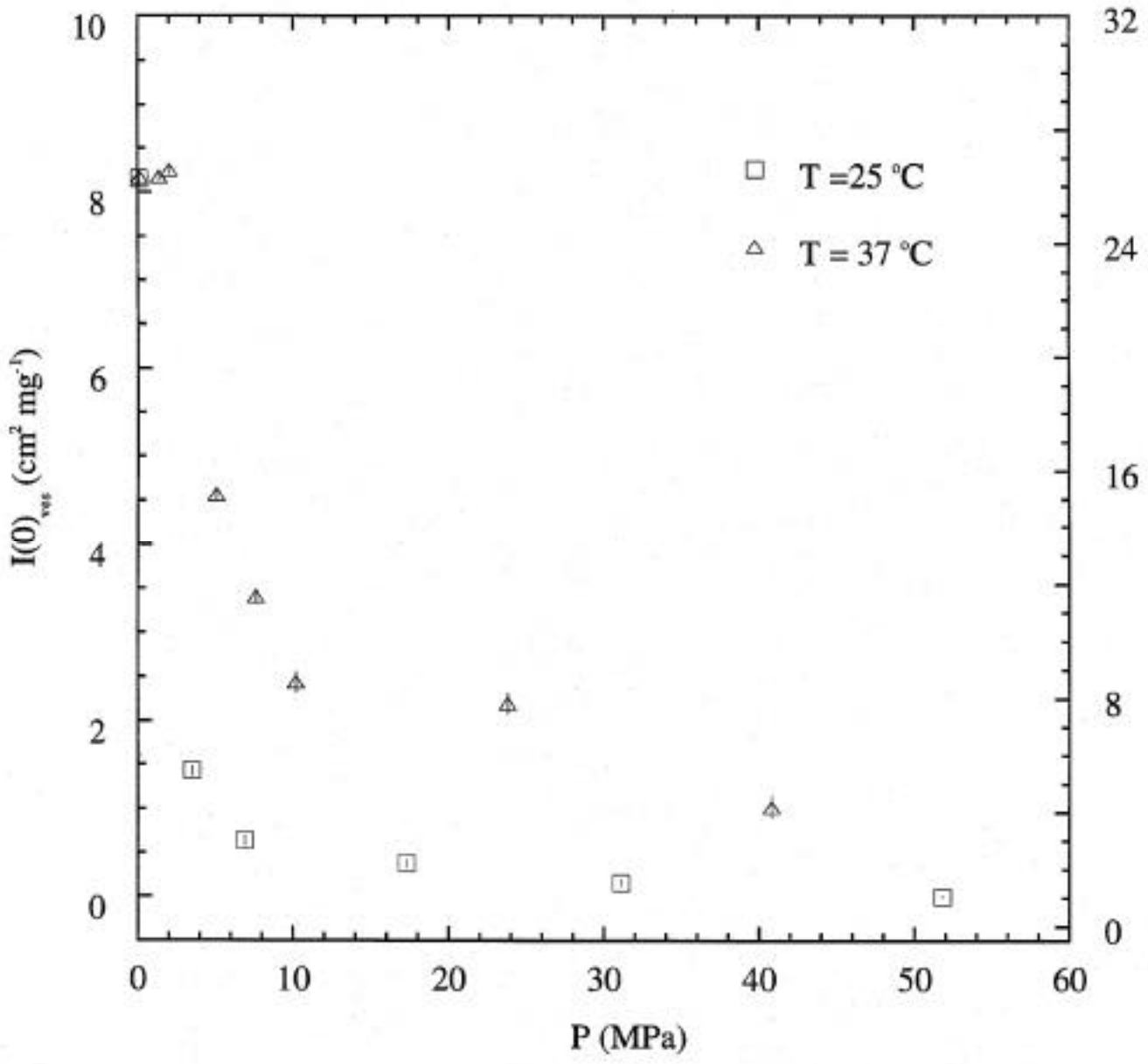
T =25 °C
T = 37 °C
I(0)vs (cm2 mg-1)
P (MPa)
0
2
4
6
8
10
0
8
16
24
32
0
10
20
30
40
50
60